

Spin-Valley Kondo Effect in Multi-electron Silicon Quantum Dots

Shiue-yuan Shiau, and Robert Joynt¹

¹*Department of Physics, University of Wisconsin,
1150 University Avenue, Madison, Wisconsin 53706*

(Dated: October 27, 2018)

We study the spin-valley Kondo effect of a silicon quantum dot occupied by \mathcal{N} electrons, with \mathcal{N} up to four. We show that the Kondo resonance appears in the $\mathcal{N} = 1, 2, 3$ Coulomb blockade regimes, but not in the $\mathcal{N} = 4$ one, in contrast to the spin-1/2 Kondo effect, which only occurs at $\mathcal{N} = \text{odd}$. Assuming large orbital level spacings, the energy states of the dot can be simply characterized by fourfold spin-valley degrees of freedom. The density of states (DOS) is obtained as a function of temperature and applied magnetic field using a finite- U equation-of-motion approach. The structure in the DOS can be detected in transport experiments. The Kondo resonance is split by the Zeeman splitting and valley splitting for double- and triple-electron Si dots, in a similar fashion to single-electron ones. The peak structure and splitting patterns are much richer for the spin-valley Kondo effect than for the pure spin Kondo effect.

I. INTRODUCTION

Single- and few-electron quantum dots (QDs) coupled to leads have been realized in the last several years¹. Their theoretical description is similar to that of a magnetic impurity in a bulk metal, a problem that has been studied for decades. It gives rise, among other things, to Kondo physics². The advantage of the QD system is that many parameters can be varied by adjusting voltages on the electrodes that surround the QD, whereas in the bulk these parameters are fixed³. One of these parameters is the total number of electrons \mathcal{N} on the QD. Of course in many cases some of the electrons on the QD can be considered as "core" electrons. This works only when the Coulomb interaction or the dot orbital level spacings are large and therefore all but one or two of the electrons residing on the closest orbital to the Fermi energy on the dot can be treated as vacuum. In this single-electron dot picture the spin-1/2 Kondo effect ensues from spin fluctuation of the dot electron spin coupled to the conduction electrons on the leads. As a result, the dot electron spin binds to an electron spin on the leads to form a spin singlet. When temperatures and magnetic field splittings are lower than the energy scale characteristic of this spin singlet, a narrow zero-bias Kondo resonance crops up in the differential conductance as a function of source-drain voltage.

For GaAs QDs^{4,5}, the Kondo effect is only observed in $\mathcal{N} = \text{odd}$ Coulomb blockade regimes. This is the only case in which it is possible for a spin singlet formed by the highest-energy electron on the dot and electrons in the leads to be the ground state, and then only provided that finite orbital spacings render it energetically favorable. No Kondo resonance is formed in $\mathcal{N} = \text{even}$ Coulomb blockade regimes, since the highest-energy dot electrons themselves will normally form a spin singlet. Thus a characteristic signature of the Kondo effect has always been this periodicity of 2 in the variable \mathcal{N} . A second characteristic signature is the magnetic field dependence. The Kondo resonance, which manifests itself as a peak

at zero voltage when the conductance is measured as a function of source-drain voltage, splits into two peaks due to the Zeeman effect. These peaks are separated by $\delta V = 2g\mu_B B$.

For Si QDs, experiments on the Kondo effect have so far been able to reach the stage of few-electron dots, but not that of single-electron ones. In a few-electron Si dot⁶, a Kondo resonance at zero bias voltage is split into two peaks by an applied magnetic field. The value of the extracted g factor is about 2.26, slightly larger than the expected 2, suggesting a possible contribution from the valley degree of freedom. No distinct periodicity has yet been observed.

We note one apparent exception to the periodicity rule in GaAs. A recent report⁷ on the spin-orbital Kondo effect in an integer-spin QD has shown a Kondo effect in an $\mathcal{N} = \text{even}$ Coulomb blockade regimes. Considering two orbital levels on the dot, the condition of a spin singlet-triplet degeneracy can be artificially achieved by tuning the magnetic field and a Kondo resonance emerges at a particular magnitude of field. When further increasing the field, this resonance splits into two peaks at a finite bias voltage, and the separation of the two peaks is twice the singlet-triplet energy difference. In perpendicular field, their difference has a much stronger field dependence than the Zeeman splitting. The smaller-scale Zeeman splitting was not observed in the data. The spin singlet-triplet Kondo effect involving two orbital levels in $\mathcal{N} = \text{even}$ regimes resembles in some respects the spin-valley Kondo effect in even-electron Si dots, the main body of this study, in the sense that the degeneracy does not come entirely from spin.

Silicon is an indirect bandgap semiconductor. The top of the valence band lies at the Γ -point, while the conduction band has six degenerate minima along the Γ - X directions. The conduction electrons in n -type silicon have therefore a sixfold degeneracy corresponding to this valley degree of freedom. Si QDs are formed in heterostructures where the active layer is a thin layer of pure silicon sandwiched between layers of $\text{Si}_{1-x}\text{Ge}_x$ alloy, which puts the silicon layer in a state of in-plane tensile strain. This

raises four of the conduction band minima by a large energy (~ 0.1 eV), leaving only a twofold valley degeneracy. This in turn is split by small effects that break the mirror symmetry (reflection through the x - y plane). This small (< 1 meV) splitting is enhanced by a perpendicular magnetic field. It can be controlled by changing electrostatic and magnetic confinement⁸. On the other hand, a two-dimensional tight-binding model⁹ predicts the possibility of valley index nonconservation during tunneling from the leads to the dots, which results in opening up additional tunneling channels between an even (odd) valley state on the leads and an odd (even) valley state on the dot, which changes significantly the features of the Kondo resonance in single-electron Si QDs. The valley mixing is made possible by the rough interfaces that confine the two dimensional electron gas (2DEG) of strained Si, in which the dot-leads system is formed.

This valley near-degeneracy is a potential source of leakage and decoherence in quantum computing schemes in which Si QDs serve as the qubits. This is an additional reason for trying to understand its consequences.

In earlier work, we showed that valley degeneracy produces a novel Kondo effect in $\mathcal{N} = 1$ Si QDs⁹. We will show below that for double-electron Si dots, there is also a Kondo resonance, which suffers both the valley and Zeeman splittings, in contrast to the Kondo resonance affected by the field-dependent singlet-triplet energy difference mentioned above⁷.

Figure 1 in Ref. 9 characterizes the four spin-valley energy levels as a function of magnetic field for a single orbital in a Si QD. This energy-level structure draws on two experiments⁸ that observed a valley splitting in Hall bars and Quantum Point Contacts (QPCs); in the first the valley splitting shows a linear dependence with applied field, in the latter the magnitude is measured to be about 1 meV. Furthermore, a finite zero-field valley splitting was observed in both experiments, in which at zero field the splitting in Hall bars is about 1.5 ± 0.6 μ eV, much smaller than in QPCs. The difference is ascribed to interface disorder^{10,11}. This level structure will again be used later to define the dot energy levels in Sec. IV.

Our aim in this paper is to describe the Kondo resonance(s) in Si QDs for $\mathcal{N} > 1$. The Kondo effect itself results from a ground state in a which the dot spin and valley states are mixed with the lead states to form a singlet ground state. The resonance in transport occurs because the resulting wave function has weight at or near the Fermi energies of both leads, leading to a zero-bias or near-zero-bias anomaly. The anomaly can be shifted and split by a magnetic field. For $\mathcal{N} = 1$, we showed that the zero-bias resonance is split by both the valley and Zeeman splittings so that there are more split peaks in non-linear $I - V$ characteristics than in the spin-1/2 Kondo effect⁹. To complete the whole picture, we continue to investigate whether there is a spin-valley Kondo effect in the $\mathcal{N} = 2, 3, 4$ Coulomb blockade regimes and if so, how the splittings occur in each regime. We use again an equation-of-motion approach to obtain the interacting

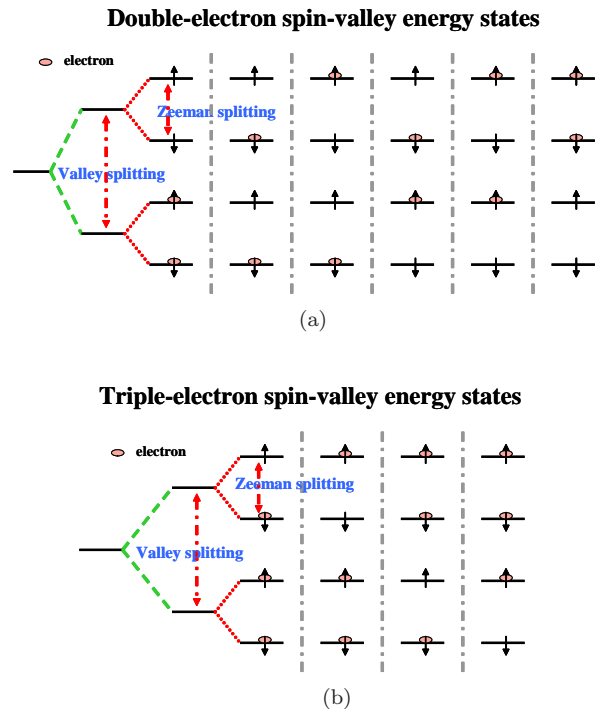


FIG. 1: When the Coulomb interaction is large, the electron occupation number \mathcal{N} is a good quantum number at weak couplings. Shown here are the six and four configurations of low-energy spin-valley dot states for the (a) $\mathcal{N} = 2$ and (b) $\mathcal{N} = 3$ regimes, respectively. The spin-valley Kondo effect is related to the \mathcal{N} -conserved many-body transitions where these dot states interact with the lead states. Note that the relative size of the valley and Zeeman splittings in the cartoon figures does not necessarily reflect every tested sample since the valley splitting is sample-dependent.

DOS that will be shown below to directly reflect the differential conductance. We assume orbital level spacings to be larger than a few times the dot Coulomb interaction U , so that the orbitals are well separated in energy. As a result, it is sufficient to only consider the single orbital closest to the Fermi energy. This condition could be satisfied in a small dot size of ~ 10 nm. Then, since the Coulomb interaction is large, the charge fluctuation is small enough for the electron occupation number \mathcal{N} to be a well-defined quantum number between the Coulomb blockade peaks. Then what needs to be taken into account is the low-energy electron configurations for each \mathcal{N} . Figure 1 demonstrates the configurations of these spin-valley energy states for $\mathcal{N} = 2, 3$ that interact with the lead states.

In the next section we describe the model and our calculation method. The results for the Kondo temperature follow in the section after that, and then we plot and discuss the DOS for various cases. Finally we summarize and give some conclusions.

II. EQUATION-OF-MOTION APPROACH

The equation-of-motion (EOM) approach has proven to be a good tool for investigating the density of states (DOS) in the Kondo effect¹². Since this quantity is the one that interests here, we shall employ this method. In particular it is able to handle arbitrary orbital structure and particle number, as well as finite temperature and the presence of a magnetic field. The basic technical

details are given in Ref. 9, so here we describe only those additional features that are required to treat the $\mathcal{N} > 1$ case.

A Hamiltonian that describes a system consisting of the single-particle energy levels of the leads, the dot, the tunneling matrix couplings that connect the levels of the leads and the dot, as well as the Coulomb interaction between electrons on the dot is the Anderson impurity model, expressed by

$$\mathcal{H} = \sum_{ik,m\sigma} \varepsilon_k c_{ikm\sigma}^\dagger c_{ikm\sigma} + \sum_{m\sigma} \varepsilon_{m\sigma} f_{m\sigma}^\dagger f_{m\sigma} + \sum_{ikm\sigma} V_{O,ik} (c_{ikm\sigma}^\dagger f_{m\sigma} + f_{m\sigma}^\dagger c_{ikm\sigma}) + \sum_{ikm\sigma} V_{X,ik} (c_{ikm\sigma}^\dagger f_{\bar{m}\sigma} + f_{\bar{m}\sigma}^\dagger c_{ikm\sigma}) + \frac{U}{2} \sum_{m'\sigma' \neq m\sigma} n_{m'\sigma'} n_{m\sigma}$$

Here the spin-1/2 index $\sigma \in \{\uparrow, \downarrow\}$, and the valley index $m \in \{e(\text{even}), o(\text{odd})\}$. Even and odd denoted the two valley states. \bar{m} is the opposite of the valley index m . The operator $c_{ikm\sigma}^\dagger (c_{ikm\sigma})$ creates (annihilates) an electron with an energy ε_k in the i lead, $i \in L, R$, while the operator $f_{m\sigma}^\dagger (f_{m\sigma})$ creates (annihilates) an electron with an energy $\varepsilon_{m\sigma}$ on the QD, connected to the leads by Hamiltonian intravalley coupling $V_{O,ik}$ and intervalley coupling $V_{X,ik}$. For perfect interfaces at the boundaries of the well, it could happen that $V_{X,ik} = 0$, i.e., that the valley index is conserved in tunneling. For real dots, we have shown that $V_{O,ik}$ and $V_{X,ik}$ are likely to be the same order of magnitude⁹. We assume that $V_{O(X)ik}$ does not depend on the spin index σ . U is the Coulomb interaction on the dot and is assumed to be independent of the valley index.

The Kondo effect can be observed by measuring the current I and likewise the differential conductance G as a function of source-drain voltage V_{sd} . Theoretically the differential conductance $G = dI/dV_{sd}$ is given by differentiating the generalized Landauer formula, given in Ref. 9. The differential conductance is approximately proportional to the interacting DOS — DOS = $-\text{Im}[\mathcal{G}_{m\sigma}(eV_{sd})]/\pi$ — given the assumption of an initially flat noninteracting DOS in the leads. Although the lead DOS and tunneling matrix elements vary with applied voltages, it is usually true that the variations are slow compared with the sharp Kondo resonance structures. When this is true, understanding the dot DOS is sufficient to identify the fine structure in the conductance near zero bias.

Thus we need to compute $\mathcal{G}_{m\sigma}(w)$, the retarded Green's function:

$$\begin{aligned} \mathcal{G}_{m\sigma}(w) &\equiv \langle\langle f_{m\sigma}, f_{m\sigma}^\dagger \rangle\rangle \\ &= -i \int_0^\infty e^{i\alpha t} \langle\{f_{m\sigma}(t), f_{m\sigma}^\dagger(0)\}\rangle dt. \end{aligned}$$

where $\alpha = w + i\delta$. We compute the equation of motion for $\mathcal{G}_{m\sigma}(w)$ in the frequency domain:

$$\begin{aligned} w \langle\langle A, B \rangle\rangle &= \langle\{A, B\}\rangle + \langle\langle [A, H], B \rangle\rangle \\ &= \langle\{A, B\}\rangle + \langle\langle A, [H, B] \rangle\rangle. \end{aligned}$$

By applying the above equation of motion to a Green's function, we obtain higher-order Green's functions on the right-hand side of the equation, which we further expand by repeating the same procedure until all second-order ($\mathcal{O}(V^2)$) contributions are preserved after the decoupling scheme¹². After some tedious but straightforward calculations, we acquire equations of motion that couple the Green's functions $\mathcal{G}_{m\sigma}(w)$, $\langle\langle f_{\bar{m}\sigma}, f_{m\sigma}^\dagger \rangle\rangle$, $\langle\langle n_l f_{m\sigma}, f_{m\sigma}^\dagger \rangle\rangle$, $\langle\langle n_{l'} f_{\bar{m}\sigma}, f_{m\sigma}^\dagger \rangle\rangle$, $\langle\langle n_l n_j f_{m\sigma}, f_{m\sigma}^\dagger \rangle\rangle$, $\langle\langle n_{l'} n_{j'} f_{\bar{m}\sigma}, f_{m\sigma}^\dagger \rangle\rangle$, $\langle\langle n_l n_j n_p f_{m\sigma}, f_{m\sigma}^\dagger \rangle\rangle$, $\langle\langle n_{l'} n_{j'} n_{p'} f_{\bar{m}\sigma}, f_{m\sigma}^\dagger \rangle\rangle$ ($\{l, j, p\} \neq m\sigma$ and $\{l', j', p'\} \neq \bar{m}\sigma$ are shorthand notations for both m and σ indices) that describe single, double, triple and quadruple occupancies, respectively. These Green's functions suffice to describe fourfold degenerate Si QDs that can host up to four electrons. They are nothing but linearly coupled matrix elements spanned by spin and valley quantum numbers, and they can be solved for by linear diagonalization in terms of their coefficients: second-order perturbation terms, integral functions, occupation numbers $\langle n_{m\sigma} \rangle$, $\langle n_l n_{m\sigma} \rangle$, $\langle n_l n_j n_{m\sigma} \rangle$, and expectation values $\langle f_{m\sigma}^\dagger f_{m\sigma} \rangle$, $\langle n_{l'} f_{m\sigma}^\dagger f_{\bar{m}\sigma} \rangle$, $\langle n_{l'} n_{j'} f_{m\sigma}^\dagger f_{\bar{m}\sigma} \rangle$ ($l', j' \neq m\sigma, \bar{m}\sigma$). It is noteworthy that some perturbation terms and the integral functions are logarithmically divergent at the Fermi energy, thereby giving rise to a zero-bias anomaly, and have to be treated carefully in the Kondo regime $T \leq T_K$ (T_K is the Kondo temperature that we will define later). Details are parallel to those in Ref. 9, so that we do not give them here, except to note the following:

First, we assume a flat and symmetric noninteracting DOS in the source and drain, so $V_{O(X),ik} = V_{O(X)}$. Since the valley index is not conserved, it is convenient

to introduce $V_O = V \cos \phi$, $V_X = V \sin \phi$. We define $V^2 = V_O^2 + V_X^2$ and $2V_O V_X = \beta V^2$ with $\beta = \sin 2\phi$ and $0 \leq \beta \leq 1$. Parameter β gauges the extent of valley index nonconservation. In other words, $\beta = 0$ implies valley index conservation, reflecting perfectly smooth interfaces of the 2DEG, whereas $\beta = 1$ the maximal valley mixing.

To compute numerical results, we use the following integral

$$\int_{-D}^D dw' \frac{f_{FD}(w')}{w - w' \pm i\delta} = -\Psi\left(\frac{1}{2} \pm \frac{w - \varepsilon_F}{2\pi iT}\right) + \ln \frac{D + w}{2\pi T} \mp \frac{i\pi}{2}$$

where the parameter D is the conduction half-bandwidth, and f_{FD} the Fermi function. $\Psi(z)$ is the digamma function that asymptotically behaves as $\ln z$ as $|z| \gg 1$. This logarithmic divergence produces a low energy scale in the Kondo regime, the domain of our interest. This scale is defined as the Kondo temperature. We also assume the self-energy term

$$\Sigma_0(w) = \sum_{ik} \frac{V^2}{w - \varepsilon_k + i\delta} \simeq -i\Gamma$$

where $\Gamma = \pi V^2/D$. This approximation is valid near the Fermi energy which is the region of most experimental interest.

The integral functions come from the correlation functions of the dot and leads after decoupling the higher-order Green's functions. By simple transformation these correlation functions can be rewritten in terms of integral functions over the Green's functions shown above, and the set of equations of motion terminates after the decoupling⁹. To compute the integral functions whose integrands contain the Green's functions, first we use the approximation adopted by Lacroix¹³ and V. Kashcheyevs *et al.*¹⁴ who assume that the integral functions are dominated by the singularity and only strongly affect the region around the Fermi energy. As a result, we can approximate, for instance, the integral function

$$\Gamma \int dw' \frac{f_{FD}(w') \mathcal{G}_{m\sigma}^*(w')}{w - w'} \simeq \Gamma \mathcal{G}_{m\sigma}^*(\varepsilon_F) \int dw' \frac{f_{FD}(w')}{w - w'} \quad (1)$$

Likewise for other integral functions.

This leads to a set of coupled integral equations for the exact Green's functions since they are functions of integrals of themselves. Our strategy here is to make a guess of the expected structures of the Green's functions, substitute them for the exact ones in all the integral functions, and iterate to self-consistency. To illustrate, we replace the Green's function $\mathcal{G}_{m\sigma}(w)$ in Eq. 1 by $G_{m\sigma}^{(at)}(w)$ in Ref.15 as the expected Green's function. If we assume $\Gamma/U \ll 1$, we find $\mathcal{G}_{m\sigma}(w)$ consistent with the features of $G_{m\sigma}^{(at)}(w)$, and equivalent to $G_{m\sigma}^{(at)}(w)$ at high temperatures where the integral functions are small and can be disregarded. Moreover, to mimic the Green's functions that feature a broad peak of width $\sim \Gamma$ centered around the discrete bare dot energy levels, each propagator $[w - \varepsilon_{m\sigma} - dU]^{-1}$ in $G_{m\sigma}^{(at)}(w)$ is given a finite spectral

width Γ_d where $d = 0, 1, 2, 3$. Γ_d 's take into account only the self-energy terms $\Sigma_0(w)$'s in each propagator. Thus we assign

$$\Gamma_0 = \Gamma, \quad \Gamma_1 = 3\Gamma, \quad \Gamma_2 = 5\Gamma, \quad \Gamma_3 = 7\Gamma.$$

This increase of spectral widths mimics real physical systems where the potential barrier gradually opens up at high energy. Despite the fact that Γ_d 's are not real spectral widths, the errors contribute only $\mathcal{O}(\Gamma^2)$ to the integral functions that already have a prefactor Γ (c.f. Eq. 1).

We shall operate under the assumption that $\Gamma/U \ll 1$, yet we are interested in the Kondo regime. Hence this approximation for the integral functions might not be valid. However, as argued by Czycholl¹², the approximated integral functions should not deviate very much from the true ones, so long as the temperature is not too far below the Kondo temperature and higher than second-order contributions can be legitimately neglected.

On the other hand the occupation numbers and other expectation values are computed by integration over the Green's functions. For instance

$$\begin{aligned} \langle n_{m\sigma} \rangle &= -\frac{1}{\pi} \int dw f_{FD}(w) \text{Im} \mathcal{G}_{m\sigma}(w). \\ \langle n_l n_{m\sigma} \rangle &= -\frac{1}{\pi} \int dw f_{FD}(w) \text{Im} \langle \langle n_l f_{m\sigma}, f_{m\sigma}^\dagger \rangle \rangle. \\ \langle f_{m\sigma}^\dagger f_{\bar{m}\sigma} \rangle &= -\frac{1}{\pi} \int dw f_{FD}(w) \text{Im} \langle \langle f_{\bar{m}\sigma}, f_{m\sigma}^\dagger \rangle \rangle. \\ \langle n_{l''} f_{m\sigma}^\dagger f_{\bar{m}\sigma} \rangle &= -\frac{1}{\pi} \int dw f_{FD}(w) \text{Im} \langle \langle n_{l''} f_{\bar{m}\sigma}, f_{m\sigma}^\dagger \rangle \rangle. \end{aligned}$$

Now that all the perturbation terms, integral functions, the occupation numbers, and other expectation values in the Green's functions have been accounted for, we proceed to iterate to self-consistency.

In Sec. III, we show the Kondo temperatures for $\mathcal{N} = 1, 2, 3$ regimes as a function of finite Coulomb interaction U , dot energy level $\varepsilon_{m\sigma}$, coupling strength Γ , and parameter β . We also present numerical results of the DOS as a function of energy, in which a Kondo resonance is found at zero bias voltage and splits when applying a magnetic field, as demonstrated in Sec. IV.

III. THE β -DEPENDENT KONDO TEMPERATURES

It is enlightening to start first with a simple case: degenerate spin-valley states. Although it is unlikely to observe a degenerate spin-valley Kondo effect in Si dots since the valley splitting is not zero even in the absence of external field, it is still useful for us to first derive the Kondo temperatures from the solutions near the Fermi energy of the real parts of the denominators in $\mathcal{G}_{m\sigma}(w)^2$. Assuming $D > |\varepsilon_{m\sigma}|, U \gg T_K$'s and at zero temperature, we obtain

$$\begin{aligned}
T_{K1}^{\pm}(\beta) &\simeq D^* \exp \frac{\pi(\varepsilon_{m\sigma} - \varepsilon_F)(\varepsilon_{m\sigma} + U - \varepsilon_F)}{(3 \pm \beta)\Gamma U} \\
T_{K2}^{\pm}(\beta) &\simeq D^* \exp \frac{\pi(\varepsilon_{m\sigma} - \varepsilon_F)(\varepsilon_{m\sigma} + U - \varepsilon_F)(\varepsilon_{m\sigma} + 2U - \varepsilon_F)}{(3 \pm \beta)\Gamma U [4/3(\varepsilon_{m\sigma} - \varepsilon_F) + (\varepsilon_{m\sigma} + 2U - \varepsilon_F)]} \\
T_{K3}^{\pm}(\beta) &\simeq D^* \exp \frac{\pi(\varepsilon_{m\sigma} + U - \varepsilon_F)(\varepsilon_{m\sigma} + 2U - \varepsilon_F)(\varepsilon_{m\sigma} + 3U - \varepsilon_F)}{(3 \pm \beta)\Gamma U [(\varepsilon_{m\sigma} + U - \varepsilon_F) + 4/3(\varepsilon_{m\sigma} + 3U - \varepsilon_F)]}
\end{aligned}$$

Where $D^* \equiv D|2\varepsilon_{m\sigma} + U - \varepsilon_F|/|D + 2\varepsilon_{m\sigma} + U|$. $T_{K1}^{\pm}(\beta)$, $T_{K2}^{\pm}(\beta)$, $T_{K3}^{\pm}(\beta)$ are the β -dependent Kondo temperatures for single, double, and triple occupancies, respectively. We have already shown⁹ that there are two Kondo temperatures—equivalent to $T_{K1}^{\pm}(\beta)$ in the infinite U limit—in single-electron Si dots if the valley index is not conserved ($\beta > 0$), and the parameter β greatly enhances one Kondo temperature while suppressing the other in a similar fashion. As a result, $T_{K1}^{\pm}(\beta)$, the largest of the two, dominates the screening of the dots. Here we show the same with double-electron and triple-electron Si dots. But when $\varepsilon_{m\sigma} + 3U < \varepsilon_F$, the spin-valley Kondo effect disappears since all energy levels are occupied and inelastic transitions are prohibited. A keen observation will give that these $T_K^{\pm}(\beta)$'s are not unrelated. Indeed, they obey a simple relation

$$\frac{1}{\ln T_{K2}^{\pm}(\beta)/D^*} \simeq \frac{1}{\ln T_{K1}^{\pm}(\beta)/D^*} + \frac{1}{\ln T_{K3}^{\pm}(\beta)/D^*} \quad (2)$$

In other words, the Kondo temperatures in the \mathcal{N} regime are influenced by the ones in the neighboring $\mathcal{N} - 1$ and $\mathcal{N} + 1$ regimes. A similar logarithmic relation was found in Ref. 16, where although a Kondo effect is produced in $\mathcal{N} = \text{even}$ regimes, it belongs to a two-level QD. Consequently it is generically different from a fourfold degenerate Si QD.

The larger Kondo temperatures $T_K^{\pm}(\beta)$'s express the energy scales where the spin-valley Kondo effect can be observed in the Kondo regime, namely, at temperatures lower than $T_K^{\pm}(\beta)$'s. The EOM approach produces a finite- U Kondo temperature $T_{K1}^{\pm}(\beta = 0)$ that is different by a prefactor $3/4$ in the exponent from the one using a scaling theory¹⁷. The discrepancy of this approach was claimed to be due to neglect of higher-order corrections¹⁸. It should therefore be stressed that $T_K^{\pm}(\beta)$'s may only show a qualitative dependence on the model parameters. Despite this defect, $T_{K1}^{\pm}(\beta)$'s computed from the EOM approach scale logarithmically the zero-bias resonance in single-electron Si QDs⁹, thereby portraying a Kondo-like effect, as will be expected the same with $T_{K2}^{\pm}(\beta)$ and $T_{K3}^{\pm}(\beta)$. The larger $T_K^{\pm}(\beta)$'s will serve as energy scales for the demonstration of the spin-valley Kondo resonances in the next section.

It is noteworthy that at zero temperature the above solutions exist except when $\varepsilon_{m\sigma} = (\varepsilon_F - U)/2$. This particular condition leads to a particle-hole symmetry. The

EOM approach fails to produce at this point an energy scale that governs the low temperature behavior. This scenario requires a special mathematical treatment^{14,19}. Regardless of its intrinsic interest, this case is not our main concern in this paper.

IV. DENSITY OF STATES

In finite magnetic field, the dot energy levels are given by $\varepsilon_{m\sigma} = \varepsilon_d + (\Delta/2 + \mu_v B)(\delta_{m,e} - \delta_{m,o}) + g\mu_B B(\delta_{\sigma,\uparrow} - \delta_{\sigma,\downarrow})$, where ε_d is the dot bare energy level and B is the applied magnetic field. Δ is the zero-field valley splitting and μ_v is the constant valley splitting slope. Note that Δ and μ_v constants are sample-dependent and may vary in actual experiments. In the following, we have taken $\mu_v = 0.1$ meV/T, slightly smaller than $g\mu_B = 0.114$ meV/T where $g = 2$. We have also chosen the parameters $\Gamma = 0.2$ meV, $D = 200\Gamma$, and $U = 40\Gamma$, which, though bringing forth small Kondo temperatures, are favorable for the purpose of illustration.

A. Degenerate spin-valley Kondo effect with valley index conservation

We have obtained in the previous section the β -dependent Kondo temperatures. It is now instructive to apply them numerically as a temperature scale to the Kondo resonance. Our task is to plot the DOS, each time tuning the bare energy level ε_d in order to shift the Fermi energy ε_F (which we set to be zero) inside the $\mathcal{N} = 1, 2, 3$ Coulomb blockade regimes, mimicking experimental manipulation of the gate voltage over the dot energy levels. Let us for a moment consider valley index conservation and full spin-valley degeneracy by disregarding the expected zero-field valley splitting. Figure 2 displays three plots of the DOS near the Fermi energy in the $\mathcal{N} = 1, 2, 3$ regimes. Not surprisingly, for odd \mathcal{N} (1,3), a narrow Kondo resonance at zero bias voltage can be seen in Fig. 2(a) and Fig.2(c). Another side peak around 2 meV in Fig. 2(a) comes from the process that two electrons are depleted from the dot simultaneously and therefore is energetically disfavored at large U . It is interesting to note that the positions and shapes of the Kondo resonances for $\mathcal{N} = 1, 3$ reflect a particle-hole symmetry. Also noteworthy is that in $\mathcal{N} = \text{odd}$ regimes

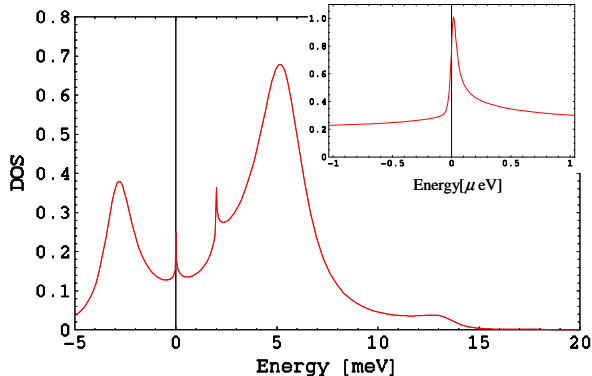
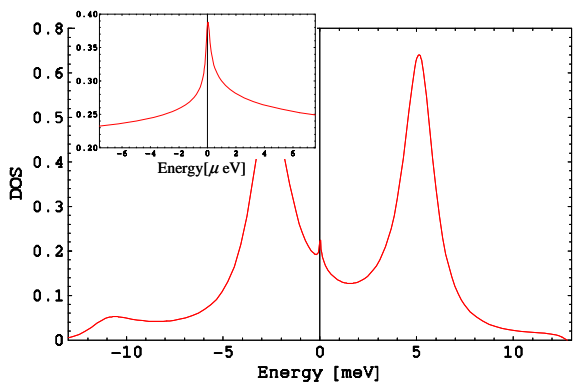
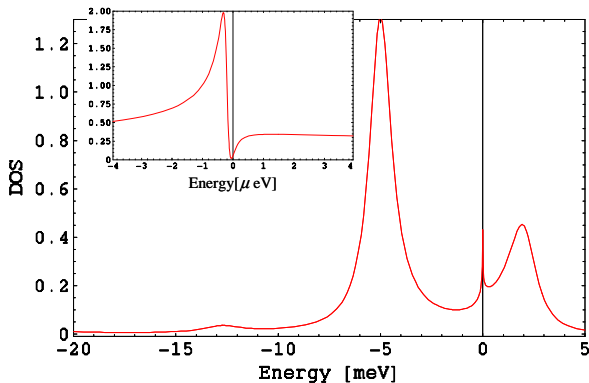
(a) DOS for $\mathcal{N} = 1$ regime.(b) DOS for $\mathcal{N} = 2$ regime.(c) DOS for $\mathcal{N} = 3$ regime.

FIG. 2: The DOS's with approximately 2(a) one, 2(b) two, 2(c) three electrons on the dot. Here the valley and Zeeman splittings are assumed to be zero. The valley index is considered conserved. In these three regimes there is a Kondo resonance at the Fermi energy, shown in the insets. To plot them we use 2(a) $\varepsilon_d = -15\Gamma$, $T/T_{K1} = 0.2$ with $T_{K1} \sim 1 \times 10^{-4}$ meV. 2(b) $\varepsilon_d = -55\Gamma$, $T/T_{K2} = 0.2$ with $T_{K2} \sim 3 \times 10^{-4}$ meV, 2(c) $\varepsilon_d = -105\Gamma$, $T/T_{K3} = 0.4$ with $T_{K3} \sim 1.6 \times 10^{-4}$ meV. The self-consistently computed occupation numbers are 2(a), $\langle n_{m\sigma} \rangle = 0.2505 \approx 1/4$; 2(b), $\langle n_{m\sigma} \rangle = 0.4831 \approx 1/2$; 2(c), $\langle n_{m\sigma} \rangle = 0.7312 \approx 3/4$.

the dot displays itself as a spin-1/2 magnetic impurity and is fully Kondo-screened by the conduction electrons on the leads. The pseudospin possessed by the valley degree of freedom behaves similarly.

On the other hand, a more symmetrical zero-bias resonance in the $\mathcal{N} = 2$ regime than the two in the $\mathcal{N} = 1, 3$ regimes is found in Fig. 2(b). This unexpected resonance is attributed to the valley degree of freedom that provides valley states for additional inelastic transitions to occur: for example, spin flips can occur even when the ground state is a singlet, if the flip is accompanied by a change in valley index. In fact, single-electron and double-electron Si QDs belong to the types of fully-screened, and under-screened Kondo effect²⁰, respectively.

A somewhat similar phenomenon of the Kondo effect can occur in a two-level quantum dot with orbital degeneracy¹⁵. By introducing an interpolative perturbative approach the Kondo effect is obtained in the $\mathcal{N} = 1, 2, 3$ regimes. However, this approach does not give an accurate estimate of the Kondo temperatures as a function of model parameters and only provides a qualitative thermal behavior. The EOM approach we have chosen here acquires similar structures for the DOS and seems more favorable to render better qualitative (if not quantitative) Kondo temperatures and Kondo resonance structures.

B. Field dependence and effect of valley index nonconservation for the $\mathcal{N} = 2$ regime

The splitting of the Kondo resonance is instructive because it disentangles clearly the interplay of all the participating low energy states and their magnetic field dependences. The peak splittings are due to the lifting of valley and spin degeneracies. Here we demonstrate the field-dependent peak splittings while taking into consideration the effect of the valley index in two extreme cases: conservation ($\beta = 0$) and full nonconservation ($\beta = 1$) of valley index. We shall particularly concentrate on the unusual Kondo peak in the $\mathcal{N} = 2$ regime.

Consider first $\beta = 0$. Fig. 3 demonstrates the peak splitting structure of double-electron Si QDs. The zero-bias peak splits into three peaks in red curve when the zero-field valley splitting $\Delta \neq 0$ and the magnetic field $B = 0$. Among these three peaks, the central splits into two peaks by the Zeeman splitting when $B \neq 0$, since it originates from a spin Kondo effect, whereas each side peak splits further into three; see the blue curve. Each peak correspond to a many-body transition. The arguments parallel those for $\mathcal{N} = 1$ ⁹: the spin-valley Kondo effect comes from spin-flip, intervalley, and intravalley inelastic transitions among the dot states in Fig. 1(a) interacting with the lead states. The valley and Zeeman splittings break the degeneracy of these dot states to produce additional peaks. We show the transition corresponding to each peak in the schematic diagrams of Fig. 3(b).

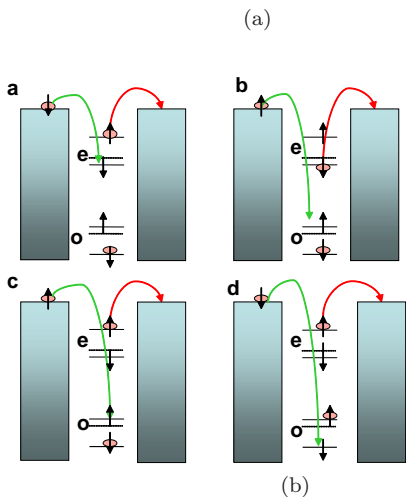
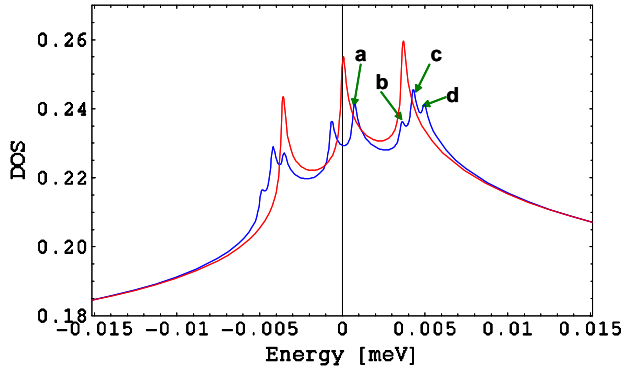
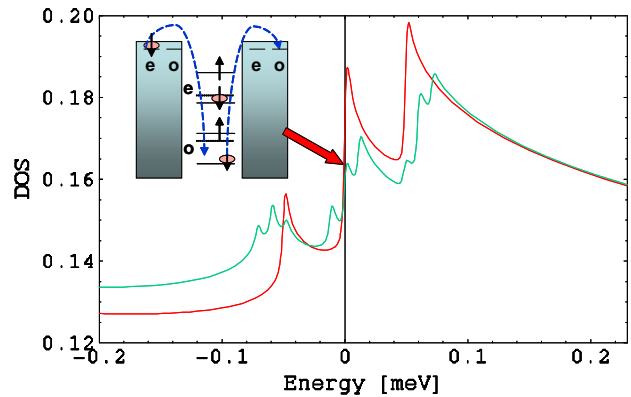


FIG. 3: (Color online) The DOS for $\mathcal{N} = 2$ is plotted with $\beta = 0$ (valley index conservation), the zero-field valley splitting $\Delta = 12 T_{K2}$ and a magnetic field $B = 0$ (red curve), 3×10^{-3} T (blue curve). The Kondo temperature $T_{K2} \sim 3 \times 10^{-4}$ meV. $T/T_{K2} = 0.2$, $\varepsilon_d = -55\Gamma$, the same for Fig. 2(b). The split peaks and their field dependences parallel those of single-electron Si QDs in Ref. 9, with similar many-body transitions in the schematic diagrams *a*, *b*, *c*, *d* producing peaks *a*, *b*, *c*, *d*, respectively.

At $\beta = 1$, we have maximal nonconservation of the valley index. For this case, Figure 4 shows an additional zero-bias peak that represents a bound state of opposite valleys, which is therefore a manifestation of the pure *valley* Kondo effect, apart from the other eight peaks already identified in Fig. 3. The transitions that generate this peak take the following course: a conduction electron at the odd (even) dot state tunnels out to the odd (even) lead state through the intravalley coupling V_O , while another electron in the even (odd) lead state tunnels into the odd (even) dot state through the intervalley coupling V_X ; see the schematic in Fig. 4. This peak height increases along with the intervalley coupling V_X , or β , which would therefore provide an experimental signature of valley index nonconservation.

As already seen in Fig. 2, the $\mathcal{N} = 1$ and $\mathcal{N} = 3$

FIG. 4: (Color online) The DOS for $\mathcal{N} = 2$ is plotted with $\beta = 1$, the zero-field valley splitting $\Delta = 10 T_{K2}^+(\beta = 1)$ and a magnetic field $B = 0$ (red curve), 5×10^{-2} T (green curve). The Kondo temperature $T_{K2}^+(\beta = 1) \sim 5 \times 10^{-3}$ meV. $T/T_{K2}^+(\beta = 1) = 0.2$, $\varepsilon_d = -55\Gamma$. Note that there emerges an extra zero-bias peak due to the effect of valley index nonconservation, compared with the peak splitting structure in Fig.3, where the valley index is conserved. It introduces another transition that involves an electron hopping between opposite valleys, as shown in the schematic diagram.



cases are rather similar. This is due to particle-hole symmetry: instead of electrons, it is the holes that tunnel in and out of the dot. The four spin-valley energy states interacting with the lead states for $\mathcal{N} = 3$ case are shown in Fig. 1(b). With these four states gradually separated by the valley and Zeeman splittings, the inelastic co-tunnelings produce a similar peak splitting structure to that for $\mathcal{N} = 1$, a case which has been exhaustively treated in Ref. 9. To avoid redundancy, we omit the plot of its DOS.

V. CONCLUSIONS

We summarize our results as follows:(a) The spin-valley Kondo effect appears as expected in the $\mathcal{N} = 1$ and $\mathcal{N} = 3$ regimes, and unexpectedly also in the $\mathcal{N} = 2$ regime, but not in the $\mathcal{N} = 4$ regime, thus yielding in general a Kondo effect unless \mathcal{N} is divisible by 4. This contrasts with the spin Kondo effect which appears only at odd \mathcal{N} . (b) Figure 2 shows an asymmetrical structure astride the Fermi energy in the position and shape of the zero-bias Kondo peaks in the $\mathcal{N} = 1$ and $\mathcal{N} = 3$ regimes. In the $\mathcal{N} = 2$ regime the peak shape is more symmetrical. (c) By applying a magnetic field, the peak splittings in the $\mathcal{N} = 2$ regimes resemble that in the $\mathcal{N} = 1$ regime. We are able to attribute each peak to its corresponding inelastic many-body transition (co-tunneling); see the cartoon schematics in Fig. 3. The rich level structure gives rise to a rich pattern of peaks.

We expect that these many-body signatures of the val-

ley degree of freedom in Si will be observed in future experiments.

Acknowledgments

We would like to thank S. Chutia, L.J. Klein, M. Friesen and M.A. Eriksson for useful discussions. This

work was supported by NSA and ARDA under ARO contract number W911NF-04-1-0389 and by the National Science Foundation through the ITR (DMR-0325634) and EMT (CCF-0523675) programs.

-
- ¹ M. Ciorga, A. S. Sachrajda, P. Hawrylak, C. Gould, P. Zawadzki, S. Jullian, Y. Feng, and Z. Wasilewski, *Phys. Rev. B* **61**, R16315 (2000).
- ² A.P. Hewson, *The Kondo Problem to Heavy Fermions*, (Cambridge Univ. Press, Cambridge, 1993), Sec. 7.2.
- ³ See, e.g., J. A. Folk, S. R. Patel, S. F. Godijn, A. G. Huibers, S. M. Cronenwett, C. M. Marcus, K. Campman and A. C. Gossard, *Phys. Rev. Lett.* **76**, 1699 (1996).
- ⁴ Sara M. Cronenwett, Tjerk H. Oosterkamp, Leo P. Kouwenhoven, *Science* **281**, 540-544 (1998).
- ⁵ D. Goldhaber-Gordon, H. Shtrikman, D. Mahalu, D. Abusch-Magder, U. Meirav, and M.A. Kastner, *Nature (London)* **391**, 156 (1998).
- ⁶ L. J. Klein, D. E. Savage, and M. A. Eriksson, *Appl. Phys. Lett.* **90**, 033103 (2007).
- ⁷ S. Sasaki *et al.*, *Nature* **405**, 764 (2000).
- ⁸ S. Goswami *et al.*, *Nature Physics* **3**, 41 (2007).
- ⁹ Shiue-yuan Shiau, Sucismita Chutia, and Robert Joynt, *Phys. Rev. B* **75**, 195345 (2007).
- ¹⁰ M. Friesen, M. A. Eriksson, and S. N. Coppersmith, *Appl. Phys. Lett.* **89**, 202106 (2006).
- ¹¹ N. Kharche, M. Prada, T. B. Boykin, and G. Klimeck, *Appl. Phys. Lett.* **90**, 092109 (2007).
- ¹² G. Czycholl, *Phys. Rev. B* **31**, 2867 (1985).
- ¹³ C. Lacroix, *J. Phys. F.* **11**, 2389 (1981).
- ¹⁴ V. Kashcheyevs, A. Aharony, and O. Entin-Wohlman, *Phys. Rev. B* **73**, 125338 (2006).
- ¹⁵ A. Levy Yeyati, F. Flores, and A. Martin-Rodero, *Phys. Rev. Lett.* **83**, 600 (1999).
- ¹⁶ M. Pustilnik, Y. Avishai, and K. Kikoin, *Phys. Rev. Lett.* **84**, 1756 (2000).
- ¹⁷ M. Eto and Y. Hada, *AIP Conf. Proc.* **850**, 1382 (2006); M. Eto, *J. Phys. Soc. Jpn.* **74**, 95 (2005).
- ¹⁸ Hong-Gang Luo, Ju-Jian Ying and Shun-Jin Wang, *Phys. Rev. B* **59**, 9710 (1999).
- ¹⁹ J. A. Appelbaum and D. R. Penn, *Phys. Rev.* **188**, 188 (1969).
- ²⁰ A. Posazhennikova, B. Bayani, and P. Coleman, *Phys. Rev. B* **75**, 245329 (2007).